Nanoscale

Accepted Manuscript

This is an *Accepted Manuscript*, which has been through the RSC Publishing peer review process and has been accepted for publication.

Accepted Manuscripts are published online shortly after acceptance, which is prior to technical editing, formatting and proof reading. This free service from RSC Publishing allows authors to make their results available to the community, in citable form, before publication of the edited article. This *Accepted Manuscript* will be replaced by the edited and formatted *Advance Article* as soon as this is available.

To cite this manuscript please use its permanent Digital Object Identifier (DOI®), which is identical for all formats of publication.

More information about *Accepted Manuscripts* can be found in the **Information for Authors**.

Please note that technical editing may introduce minor changes to the text and/or graphics contained in the manuscript submitted by the author(s) which may alter content, and that the standard **Terms & Conditions** and the **ethical guidelines** that apply to the journal are still applicable. In no event shall the RSC be held responsible for any errors or omissions in these *Accepted Manuscript* manuscripts or any consequences arising from the use of any information contained in them.

Cite this: DOI: 10.1039/c0xx00000x

www.rsc.org/xxxxxx

ARTICLE TYPE

Janus Nanobelt: Fabrication, Structure and Enhanced Magnetic-Fluorescent Bifunctional Performance

Qianli Ma, Wensheng Yu, Xiangting Dong,* Jinxian Wang, and Guixia Liu

Received (in XXX, XXX) Xth XXXXXXXXX 20XX, Accepted Xth XXXXXXXXX 20XX
DOI: 10.1039/b000000x

A new nanostructure of magnetic-fluorescent bifunctional Janus nanobelts with Fe_3O_4/PMMA as one half side and Tb(BA)$_3$phen/PMMA as the other half side has been successfully fabricated by specially designed parallel spinneret electrospinning technology. The morphology and properties of the final products were investigated in detail by X-ray diffractometry (XRD), scanning electron microscopy (SEM), energy dispersive spectrometry (EDS), biological microscopy (BM), vibrating sample magnetometry (VSM) and fluorescence spectroscopy. The results revealed that the [Fe_3O_4/PMMA]//[Tb(BA)$_3$phen/PMMA] magnetic-fluorescent bifunctional Janus nanobelts possess superior magnetic and fluorescent properties due to their special nanostructure. Compared with Fe_3O_4/Tb(BA)$_3$phen/PMMA composite nanobelts, the magnetic-fluorescent bifunctional Janus nanobelts provided better performance. The new type magnetic-fluorescent bifunctional Janus nanobelts have potential applications in novel nano-bio-label materials, drug target delivery materials and future nanodevice due to their excellent magnetic-fluorescent properties, flexibility and insolubility. Moreover, the construct technique for the Janus nanobelts is of universal significance to fabricate other multifunctional Janus nanobelts.

Introduction

Since magnetic-fluorescent nanomaterials have been applied in medical diagnostics, optical imaging, nanodevice, etc[1,2], many researches are focused on their preparations and properties in recent years. In general, Fe_3O_4, $MnFe_2O_4$, $CoFe_2O_4$ or $NiFe_2O_4$ is adopted as the magnetic core of the magnetic-fluorescent bifunctional nanoparticles (NPs), while quantum dot, rare earth (RE) compound or fluorescent dye is used as the luminescent shell[3-8]. In order to obtain new morphologies of magnetic-fluorescent nanomaterials, the fabrication of one-dimensional (1D) magnetic-fluorescent nanomaterials is an urgent subject of study.

Electrospinning is an outstanding technique to process viscous solutions or melts into continuous fibers or belts with 1D nanostructure[9-11]. This method not only attracts extensive academic investigations, but is also applied in many areas such as filtration[12], optical and chemical sensors[13], biological scaffolds[14], electrode materials[15], and nanocables[16,17]. Very recently, Fe_2O_3/Eu(DBM)$_3$(Bath)/PVP composite nanofibers[18] and Fe_3O_4/Eu(BA)$_3$phen/PVP composite nanofibers[19] were prepared via electrospinning. It has been proved that the Fe_3O_4 or Fe_2O_3 will greatly decrease the luminescence of RE compounds if they are directly blended with the RE luminescent compounds. Therefore, RE complex should be effectively isolated to avoid direct contact with Fe_3O_4 NPs if the strong luminescence of the magnetic-fluorescent bifunctional nanofibers is achieved. Our previous research has demonstrated that the nanostructure of coaxial nanofibers can help to realize this academic idea, and the coaxial nanofibers simultaneously exhibited excellent magnetic and fluorescent properties[20].

Nanobelt has attracted increasing interest of scientists owing to its anisotropy, large width-thickness ratio, unique optical, electrical and magnetic properties. We have fabricated magnetic-fluorescent bifunctional Fe_3O_4/RE complex/PMMA composite nanobelts in our previous study[21], and the composite nanobelts also suffered heavy losses in fluorescent intensity when Fe_3O_4 NPs were directly mixed with the RE luminescent compounds. In the procedure of seeking a way to ultimately reduce the impact of Fe_3O_4 NPs on the fluorescent property of the magnetic-fluorescent bifunctional nanobelts, we were inspired by the reports on the Janus particles[22-25]. 'Janus' is the name of an ancient Roman God, who has two faces peering into the past and the future. Named after this Roman God, Janus particles have two distinguished surfaces/chemistries on the two sides. Pierre-Gilles de Gennes, Nobel Prize in Physics winner, made the Janus particles known to the scientific community. Upon the unique feature of the asymmetry dual-sided Janus structure, we designed and fabricated magnetic-fluorescent bifunctional [Fe_3O_4/PMMA]//[Tb(BA)$_3$phen/PMMA] Janus nanobelts (for short, denoted the [Fe_3O_4/PMMA]//[Tb(BA)$_3$phen/PMMA] Janus nanobelts as M//F Janus nanobelts) with new 1D structure in this paper, and a new kind of spinning spinneret was designed and manufactured to fabricate this novel nanostructure. Of the M//F Janus nanobelt, its one half side is composed of template PMMA containing Fe_3O_4 NPs (magnetic half side), and the other half side consists of PMMA containing RE complexes (fluorescent half side). This new 1D nanostructure can successfully realize the effective separation of Fe_3O_4 NPs from the RE complexes and this new morphology of bifunctional nanobelts will be obtained with excellent magnetism and luminescence. To the best of our knowledge, the new structured Janus nanobelts have not been found in any literature. The structure, fluorescence and magnetism of the Janus nanobelts were also studied.

Experimental Sections

Chemicals

Methylmethacrylate (MMA), benzoylperoxide (BPO), Tb_4O_7, benzoic acid (BA), 1,10-phenanthroline (phen), $FeCl_3{\cdot}6H_2O$, $FeSO_4{\cdot}7H_2O$, NH_4NO_3, polyethyleneglycol (PEG, Mw≈20,000), ammonia, anhydrous ethanol, $CHCl_3$, and DMF are of analytical grade and directly used as received without further purification. The purity of Tb_4O_7 is 99.99 %. Deionized water is homemade.

Nanoscale Accepted Manuscript

Preparation of Fe_3O_4 Nps by coprecipitation method

Fe_3O_4 NPs were obtained via a facile coprecipitation synthetic method[26], and PEG was used as the protective agent to prevent the particles from aggregation. One typical synthetic procedure was as follows: 5.4060 g of $FeCl_3{\cdot}6H_2O$, 2.7800 g of $FeSO_4{\cdot}7H_2O$, 4.0400 g of NH_4NO_3, and 1.9000 g of PEG were added into 100 mL of deionized water to form uniform solution under vigorous stirring at 50 °C. To prevent the oxidation of Fe^{2+}, the reactive mixture was kept under argon atmosphere. After the mixture had been bubbled with argon for 30 min, 0.1 mol/L of $NH_3{\cdot}H_2O$ was added dropwise into the mixture to adjust the pH value above 11. Then the system was continuously bubbled with argon for 20 min at 50 °C, and a black precipitate was formed. The precipitates were collected from the solution by magnetic separation, washed with deionized water for three times, and then dried at 60 °C for 12 h in an electric vacuum oven.

Synthesis of $Tb(BA)_3$phen complexes

$Tb(BA)_3$phen powder was synthesized according to the traditional method as described in the reference[27]. 1.8693 g of Tb_4O_7 was dissolved in 10 mL of concentrated nitric acid and then crystallized by evaporation of excess nitric acid and water, and $Tb(NO_3)_3{\cdot}6H_2O$ was acquired. $Tb(NO_3)_3$ ethanol solution was prepared by adding 10 mL of anhydrous ethanol into the above $Tb(NO_3)_3{\cdot}6H_2O$. 1.8320 g of benzoic acid (BA) and 0.9910 g of phenanthroline (phen) were dissolved in 100 mL of ethanol. The $Tb(NO_3)_3$ solution was then added into the solution of BA and phen with magnetic agitation for 3 h at 60 °C. The precipitate was collected by filtration and dried at 60 °C for 12 h.

Preparation of PMMA

PMMA was prepared by oxidative polymerization of MMA[28]. 100 mL of methylmethacrylate and 0.1000 g of benzoylperoxide were mixed in a 250-mL three-necked flask with a backflow device and stirred vigorously at 90-95 °C. When the viscosity of the mixture solution reached up to a certain value just like that of glycerol, the heating was stopped and then natural cooling down to room temperature. The obtained gelatinous solution was loaded into test tubes, and the influx height was 5-7 cm. After that, the tubes were put in an electric vacuum oven at 50 °C for 48 h, the gelatinous solution was solidified. At last, the temperature in the oven was raised to 110 °C for 2 h to terminate the reaction.

Preparations of spinning solutions for fabricating Janus nanobelts

Two different kinds of spinning solutions were prepared to fabricate Janus nanobelts. The spinning solution for the one half side of Janus nanobelt was composed of oleic acid modified Fe_3O_4 NPs, PMMA, $CHCl_3$ and DMF (spinning solutions I). To improve the monodispersity, stability and solubility of Fe_3O_4 NPs in the spinning solution, the as-prepared Fe_3O_4 NPs were coated with oleic acid as below: per 1.0000 g of the as-prepared Fe_3O_4 NPs were ultrasonically dispersed in 50 mL of deionized water for 20 min. The suspension was heated to 80 °C under argon atmosphere with vigorous mechanical stirring for 30 min and then 0.5 mL of oleic acid was slowly added. Reaction was stopped after heating and stirring the mixture for 40 min. The precipitates were collected from the solution by magnetic separation, washed with ethyl alcohol for three times, and dried in an electric vacuum oven at 60 °C for 6 h. The dosages of deionized water and oleic acid were changed proportionately with the used amount of Fe_3O_4 NPs. Then, all of the products were dispersed in 9.3750 g of $CHCl_3$ and 0.6250 g of DMF to form a stable emulsion, and then 0.5000 g of PMMA was added into the emulsion with stirring as a viscosity improver and template for electrospinning process. In order to investigate the impact of Fe_3O_4 NPs on the magnetic and fluorescent properties of the Janus nanobelts, various amounts of Fe_3O_4 NPs were introduced into the spinning solutions I.

Another spinning solution for the other half side of Janus nanobelt consisted of $Tb(BA)_3$phen, PMMA, $CHCl_3$ and DMF (spinning solutions II). In order to find the optimum content of $Tb(BA)_3$phen in the Janus nanobelts to endow the Janus nanobelts strongest fluorescent intensity, different amounts of $Tb(BA)_3$phen were added into the spinning solutions II. The compositions and contents of these spinning solutions were listed in Table 1.

Table 1 Compositions of spinning solutions

Compositions / Spinning solutions	Fe_3O_4 NPs/g	$Tb(BA)_3$phen/g	PMMA/g	DMF/g	$CHCl_3$/g
I-1	3.0000	0	0.5000	0.6250	9.3750
I-2	2.0000	0	0.5000	0.6250	9.3750
I-3	1.0000	0	0.5000	0.6250	9.3750
I-4	0.5000	0	0.5000	0.6250	9.3750
II-1	0	0.0250	0.5000	0.6250	9.3750
II-2	0	0.0500	0.5000	0.6250	9.3750
II-3	0	0.0750	0.5000	0.6250	9.3750
II-4	0	0.1000	0.5000	0.6250	9.3750

Electrospinning equipments for fabricating Janus nanobelts

We invented a specially designed parallel spinneret to fabricate Janus nanobelts. As shown in Figure 1, the spinneret is composed of a pair of stainless steel needles assembled side by side and fixed by a plastic nozzle. The two spinning solutions could have formed asymmetry dual-sided structure before they flow to the tip of the plastic nozzle. As a result, the Taylor cone and the final products could remain this asymmetry dual-sided structure—Janus structure.

Nanoscale Accepted Manuscript

This journal is © The Royal Society of Chemistry [year]

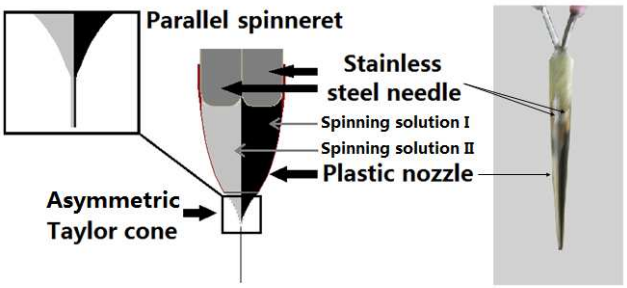

Fig. 1 Schematic diagram (left) and photograph (right) of the specially designed parallel spinneret

The equipments for electrospinning process are presented in Figure 2. The spinning solutions I and II were loaded into each plastic syringe, respectively. A flat iron net was put about 18 cm away from the tip of the plastic nozzle as a nanobelts collector. A positive direct current (DC) voltage of 6 kV was applied between the spinneret and the collector to generate stable, continuous PMMA-based Janus nanobelts at 24-26 °C, and the relative humidity was 48-52 %. The flow rate of each spinning solution is ca. 0.06 mL·min^{-1}.

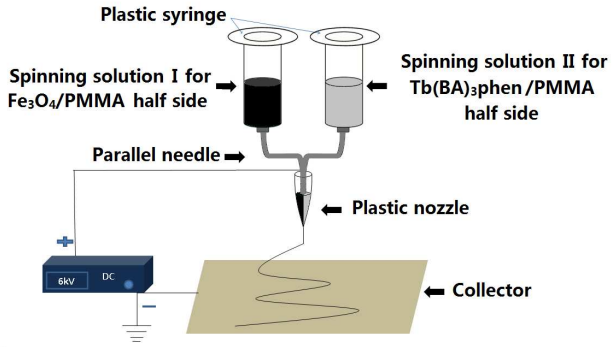

Fig. 2 Schematic diagrams of the equipments for electrospinning Janus nanobelts

Characterization

The as-prepared Fe_3O_4 NPs and M//F Janus nanobelts were identified by an x-ray powder diffractometer (XRD, Bruker, D8 FOCUS) with Cu Kα radiation. The operation voltage and current were kept at 40 kV and 20 mA, respectively. The morphology and internal structure of the Janus nanobelts were observed by a field emission scanning electron microscope (FESEM, XL-30) and a biological microscope (BM, CVM500E), respectively. The elements analysis for the Janus nanobelts was performed by an energy dispersive spectrometer (EDS, Oxford ISIS 300) attached to the FESEM. The fluorescent properties of the samples were investigated by a Hitachi fluorescence spectrophotometer F-7000. Then, the magnetic performance of Fe_3O_4 NPs, Janus nanobelts was measured by a vibrating sample magnetometer (VSM, MPMS SQUID XL). All the measures were performed at room temperature.

Results and Discussion

Phase identification

The phase compositions of the Fe_3O_4 NPs and M//F Janus nanobelts (fabricated using spinning solutions I-1 and II-2) were characterized by means of XRD analysis, as shown in Figure 3. The XRD patterns of the as-prepared Fe_3O_4 NPs are conformed to the cubic structure of Fe_3O_4 (PDF 74-0748), and no characteristic peaks are observed for other impurities such as Fe_2O_3 and FeO(OH). The diffraction peak of the amorphous PMMA ($2\theta \approx 15°$) could also be observed. These results demonstrate that the Janus nanobelts contain Fe_3O_4 NPs and the amorphous PMMA.

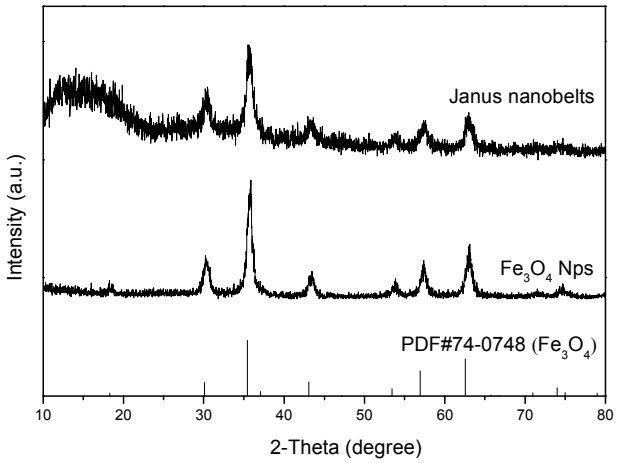

Fig. 3 XRD patterns of the Fe_3O_4 NPs and M//F Janus nanobelts

Morphology and structure

The morphology of the as-prepared Fe_3O_4 NPs was observed by means of SEM and TEM, as presented in Figure 4a. The as-synthesized spherical Fe_3O_4 NPs have a narrow size distribution and the diameter of the NPs is 9.06 ± 0.79 nm (Figure 4b). The morphology and structure of M//F Janus nanobelts (fabricated using spinning solutions I-1 and II-2) were characterized by the combination of SEM, BM and EDS line scan analyses. As shown in Figure 4c, the width of the Janus nanobelts is 15.06 ± 0.75 μm (Figure 4d) and the thickness is less than a micrometer, and some particle aggregates are faintly visible in one half side of the Janus nanobelts.

Depending on the transmission light of the BM, the inner structure of the M//F Janus nanobelts can be evidently observed. As revealed in Figure 4e, an obvious asymmetry dual-sided structure can be seen in the M//F Janus nanobelts. The Janus nanobelts is composed of a dark-colored half side (Fe_3O_4/PMMA) and a transparent half side (Tb(BA)$_3$phen/PMMA). To illustrate the advantages of the nanostructure of the magnetic-fluorescent bifunctional Janus nanobelts, Fe_3O_4/Tb(BA)$_3$phen/PMMA composite nanobelts, as the contrast sample, were also fabricated by mixing spinning solution I-1 and spinning solution II-2 together at the volume ratio of 1:1 and electrospun via the traditional single-nozzle electrospinning method. This fabrication of the Fe_3O_4/Tb(BA)$_3$phen/PMMA composite nanobelt is an easy way to realize the preparation of the magnetic-fluorescent bifunctional nanomaterials. The BM image of the Fe_3O_4/Tb(BA)$_3$phen/PMMA composite nanobelts was shown in Figure 4f, one can see that the Fe_3O_4 NPs are distributed throughout the Fe_3O_4/Tb(BA)$_3$phen/PMMA composite nanobelts.

In order to further demonstrate the asymmetry dual-sided structure of the M//F Janus nanobelts, EDS line scan analysis were performed, as presented in Figure 4g, where Tb and Fe elements represent Tb(BA)$_3$phen and Fe_3O_4, respectively. It is found that Tb and Fe elements are only existed in each one half side of the M//F Janus nanobelts. These results are well consistent with the asymmetry dual-sided structure of the Janus nanobelts.

From the SEM and BM observation and EDS line scan analysis, we can safely conclude that the M//F Janus nanobelts have been successfully fabricated.

Nanoscale Accepted Manuscript

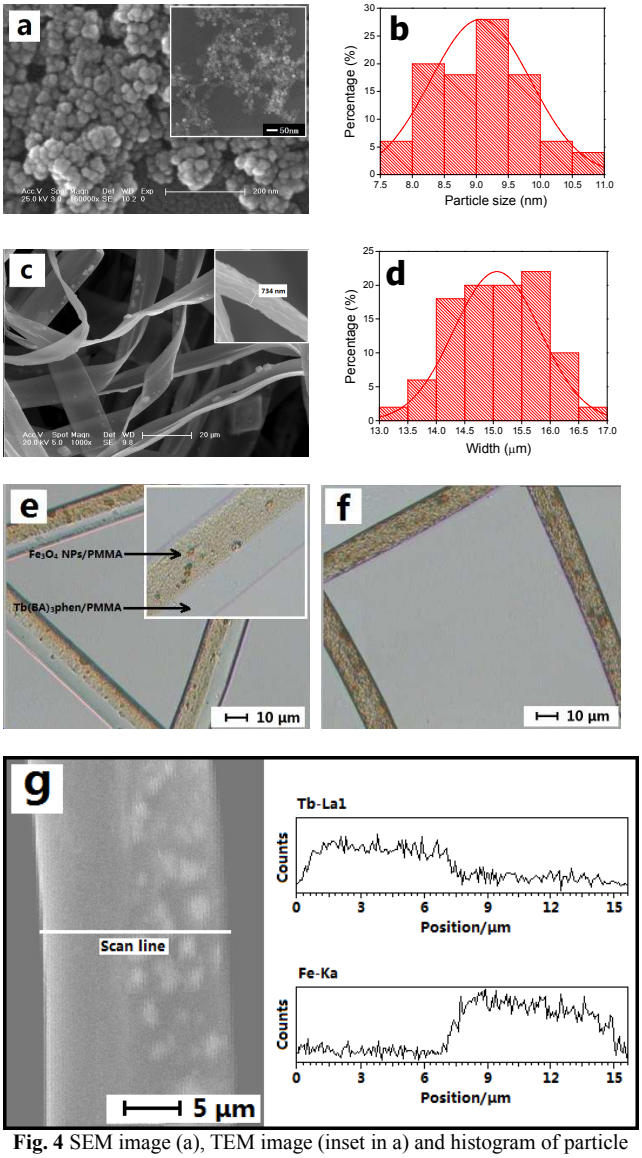

Fig. 4 SEM image (a), TEM image (inset in a) and histogram of particle size (b) of Fe_3O_4 NPs; SEM image (c), histogram of width (d) and BM image (e) of M//F Janus nanobelts; BM image (f) of Fe_3O_4/Tb(BA)$_3$phen/PMMA composite nanobelts; and EDS line scan analysis (g) of a M//F Janus nanobelt

Fluorescent performance

In order to obtain the optimum percentage of Tb(BA)$_3$phen to PMMA, a series of Tb(BA)$_3$phen/PMMA nanobelts were fabricated by using spinning solutions from II-1 to II-4 via traditional single-nozzle electrospinning process. As revealed in Figure 5, the fluorescence intensity increases at the beginning and then decreases with adding more Tb(BA)$_3$phen. The highest fluorescent intensity is acquired when the mass percentage of Tb(BA)$_3$phen to PMMA is 10 % (fabricated using spinning solutions II-2). The left part of Figure 5 demonstrates the excitation spectra of the samples monitored at 544 nm. Broad excitation bands extending from 200 to 400 nm are observed in various samples. The peak at 333 nm are assigned to the $\pi \rightarrow \pi^*$ electron transition of the ligands. As shown in the right part of Figure 5, characteristic emission peaks of the Tb^{3+} ions are observed under the excitation of 333-nm ultraviolet light. They are ascribed to the energy level transitions of the $^5D_4 \rightarrow {}^5F_6$ (495 nm), $^5D_4 \rightarrow {}^5F_5$ (544 nm), $^7D_4 \rightarrow {}^5F_4$ (588 nm), $^5D_4 \rightarrow {}^7F_3$ (624 nm), respectively. The $^5D_4 \rightarrow {}^5F_5$ hypersensitive transition at 544 nm is the predominant emission. The results indicate that the composite nanobelts containing 10 % Tb(BA)$_3$phen have the strongest fluorescence intensity. The RE complexes doped polymer has an optimum content of RE complexes in most cases. When the doping concentration of the RE complexes exceeds the optimum content, the fluorescent intensity of the RE complexes doped polymer is usually decreased because of quenching concentration[29]. Therefore, the mass percentage of Tb(BA)$_3$phen to PMMA settled at 10 % was adopted to prepare the fluorescent half side of the M//F Janus nanobelts.

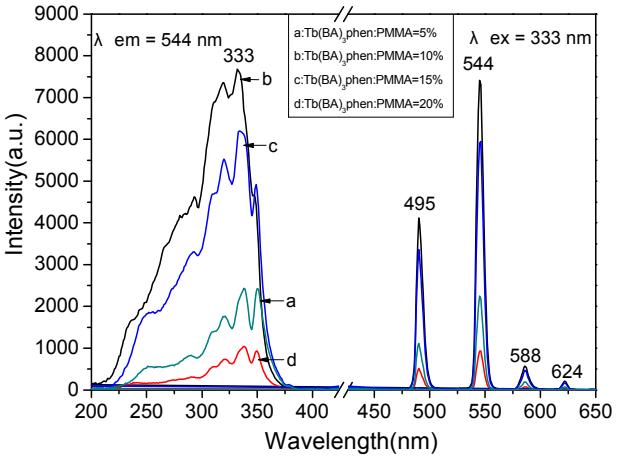

Fig. 5 Excitation spectra (left) and emission spectra (right) of Tb(BA)$_3$phen/PMMA composite nanobelts containing different mass percentage of Tb(BA)$_3$phen complexes

The fluorescence decay curves of Tb(BA)$_3$phen complexes and Tb(BA)$_3$phen/PMMA nanobelts containing different mass percentage of Tb(BA)$_3$phen complexes, as seen from Figure 6, are used to calculate the lifetime and to investigate the fluorescence dynamics of these samples. The samples are excited by 333 nm and monitored at 544 nm, and the curves can be well-fitted into a double-exponential function, and the obtained average lifetime values (τ/ms) of the samples are shown in Figure 6. It is obvious that the fluorescence lifetime for the $^5D_4 \rightarrow {}^5F_5$ transition in the Tb(BA)$_3$phen/PMMA nanobelts becomes longer than that in the pure Tb(BA)$_3$phen complexes, and the fluorescence lifetime is decreased with an increase in the complex content in the Tb(BA)$_3$phen/PMMA nanobelts. Similar conclusions about RE complexes doped polymers can be found in literatures[30,31]. When the complex content is low, most of the Tb(BA)$_3$phen complexes uniformly disperse in the Tb(BA)$_3$phen/PMMA nanobelts as molecular clusters and/or nanoparticles, which enhances the fluorescence of individual Tb(BA)$_3$phen molecules and considerably prolongs the fluorescence lifetime. With the increase of the Tb(BA)$_3$phen content, some aggregates are formed in the polymer matrix. The exciton migration between the Tb(BA)$_3$phen molecules shortens the fluorescence lifetime of Tb(BA)$_3$phen/PMMA nanobelts.

Nanoscale Accepted Manuscript

This journal is © The Royal Society of Chemistry [year]

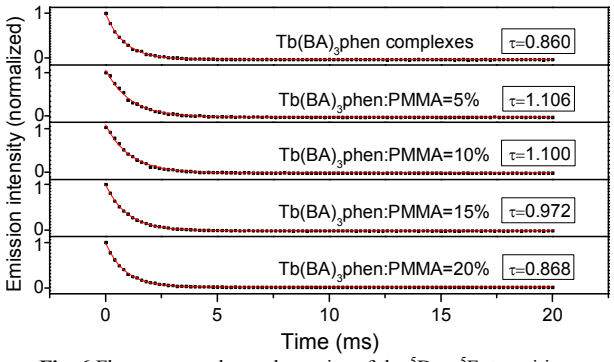

Fig. 6 Fluorescence decay dynamics of the $^5D_4 \rightarrow {}^5F_5$ transitions (λ_{em} = 544 nm) in pure $Tb(BA)_3phen$ complexes and $Tb(BA)_3phen$/PMMA composite nanobelts containing different mass percentage of $Tb(BA)_3phen$ complexes

Figure 7b gives the fluorescent emission spectra (excited by 333 nm) of M//F Janus nanobelts containing different amounts of Fe_3O_4 NPs. The fluorescent half sides of the Janus nanobelts were fabricated using spinning solution II-2, and the magnetic half sides of them were fabricated using spinning solution I-1 (Fe_3O_4: PMMA = 6: 1), I-2 (Fe_3O_4: PMMA = 4: 1), I-3 (Fe_3O_4: PMMA = 2: 1) and I-4 (Fe_3O_4: PMMA = 1: 1), respectively. One can see from comparing emission spectrum a to d in Figure 7b that the emission intensity of the M//F Janus nanobelts is decreased with the increase of the amount of Fe_3O_4 NPs introduced into the magnetic half sides of the Janus nanobelts. This phenomenon can be explained by the light absorption of Fe_3O_4 NPs which were mixed into the nanobelts[32]. From the absorbance spectrum of Fe_3O_4 NPs illustrated in Figure 7a, it is seen that the Fe_3O_4 NPs absorb light at ultraviolet wavelengths (<400 nm) much more strongly than visible range (400-700 nm). Thus, the exciting light (333 nm) and emitting light (495, 544, 588 and 624 nm) are absorbed by the Fe_3O_4/PMMA half side and the intensities are decreased. Furthermore, the light absorption would become stronger with introducing more Fe_3O_4 NPs into the magnetic half side.

In order to further discuss the variation trend, the intensities of every emission peak of each sample versus different samples were plotted in the inset of Figure 7b. The decreasing rate of the fluorescent intensity is reduced with the increase of the amount of Fe_3O_4 NPs introduced into the magnetic half side. The possible reason is that the blackness of the magnetic half side would gradually reach saturation, and the light absorption of the magnetic half side is nearly maximized with more Fe_3O_4 NPs introduced into the Janus nanobelts.

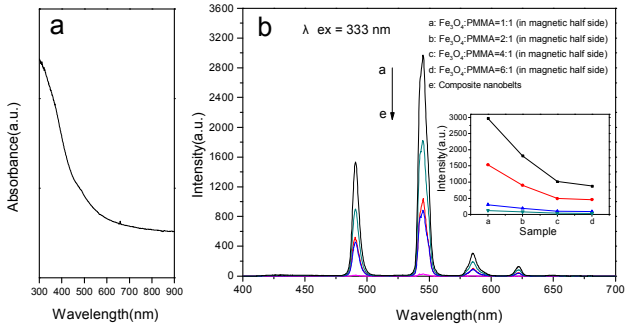

Fig. 7 UV-vis absorbance spectrum of Fe_3O_4 NPs (a) and comparison of emission spectra of M//F Janus nanobelts containing different mass ratios of Fe_3O_4 NPs and Fe_3O_4/$Tb(BA)_3phen$/PMMA composite nanobelts (b)

Figure 8 shows the fluorescence decay curves for the M//F Janus nanobelts with the mass ratio of Fe_3O_4 to PMMA as 6:1 in magnetic half side and Fe_3O_4/$Tb(BA)_3phen$/PMMA composite nanobelts. The average lifetime value of the tested M//F Janus nanobelts is 1.087 ms, which is close to that of the $Tb(BA)_3phen$/PMMA nanobelts with the mass percentage of $Tb(BA)_3phen$ to PMMA as 10% (1.100 ms), meaning that the dispersed states of $Tb(BA)_3phen$ complexes in these two kinds of nanobelts are similar. The average lifetime value of the Fe_3O_4/$Tb(BA)_3phen$/PMMA composite nanobelts (1.133 ms) is relatively longer than that of the tested M//F Janus nanobelts, which can be attributed to the fact that the $Tb(BA)_3phen$ complexes in composite nanobelts are further divided by Fe_3O_4 NPs.

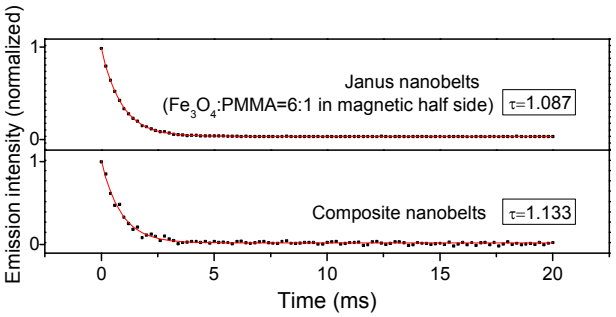

Fig. 8 Fluorescence decay dynamics of the $^5D_4 \rightarrow {}^5F_5$ transitions (λ_{em} = 544 nm) in M//F Janus nanobelts with the mass ratio of Fe_3O_4 to PMMA as 6:1 in magnetic half side and Fe_3O_4/$Tb(BA)_3phen$/PMMA composite nanobelts

From the comparison of the samples d and e in Figure 7b, it is found that the emission intensity of the Fe_3O_4/$Tb(BA)_3phen$/PMMA composite nanobelts is much weaker than that of the M//F Janus nanobelts, which seriously hinders its practical application. This heavy loss in fluorescent emission intensity is caused by the strong light absorption of the dark-colored Fe_3O_4 NPs when Fe_3O_4 NPs and $Tb(BA)_3phen$ were mixed together. As illustrated in Figure 9, because the Fe_3O_4 NPs are distributed over the whole region of the Fe_3O_4/$Tb(BA)_3phen$/PMMA composite nanobelts, the exciting light has to pass through many Fe_3O_4 NPs to reach the $Tb(BA)_3phen$ complex. In this process, a large part of the exciting light has been absorbed by Fe_3O_4 NPs, and thus the exciting light is much weakened before it reaches the $Tb(BA)_3phen$ complex. Similarly, the emitting light emitted by the $Tb(BA)_3phen$ complex also has to pass through the Fe_3O_4 NPs and is absorbed by Fe_3O_4 NPs. Consequently, the emitting light is severely weakened. For the M//F Janus nanobelts, the Fe_3O_4 NPs and $Tb(BA)_3phen$ complex are separated in their own domains of the nanobelts so that the exciting light and emitting light in the $Tb(BA)_3phen$/PMMA domain will be affected little by the Fe_3O_4 NPs. The overall result is that the M//F Janus nanobelts possess much higher fluorescent intensity than the Fe_3O_4/$Tb(BA)_3phen$/PMMA composite nanobelts. Thus, Janus nanobelts possess strong fluorescent emission intensity through isolating the $Tb(BA)_3phen$ from Fe_3O_4 NPs.

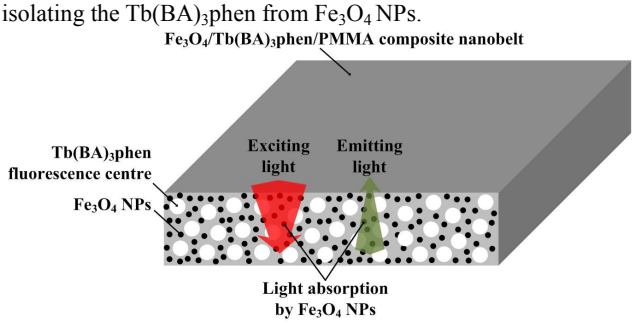

Nanoscale Accepted Manuscript

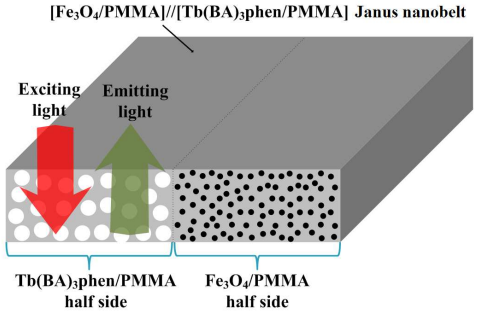

Fig. 9 Schematic diagrams of the situation of the exciting light and emitting light in the Fe_3O_4/Tb(BA)$_3$phen/PMMA composite nanobelt and M//F Janus nanobelt

Magnetic property

The typical hysteresis loops for Fe_3O_4 NPs, M//F Janus nanobelts containing different mass ratios of Fe_3O_4 NPs and Fe_3O_4/Tb(BA)$_3$phen/PMMA composite nanobelts are shown in Figure 10, and their saturation magnetizations are listed in Table 2. It is well known that the saturation magnetization of a magnetic composite material depends on the mass percentage of the magnetic substance in the magnetic composite material[33,34]. It is found that the saturation magnetization of the M//F Janus nanobelts is increased with the increase of the amount of Fe_3O_4 NPs introduced into the magnetic half side. The saturation magnetization of the Fe_3O_4/Tb(BA)$_3$phen/PMMA composite nanobelts is 32.15 emu·g^{-1}, which is close to that of the Janus nanobelts marked b (32.61 emu·g^{-1}) in Figure 10 because they were both prepared by spinning solution I-1 and spinning solution II-2. Combined the analyses of magnetism and fluorescence, it is found that the M//F Janus nanobelts have the close magnetic property to the Fe_3O_4/Tb(BA)$_3$phen/PMMA composite nanobelts. Moreover, the fluorescent intensity of the Janus nanobelts is much higher than that of the composite nanobelts, demonstrating that the novel Janus nanobelts have better magnetic-fluorescent performance than the composite nanobelts.

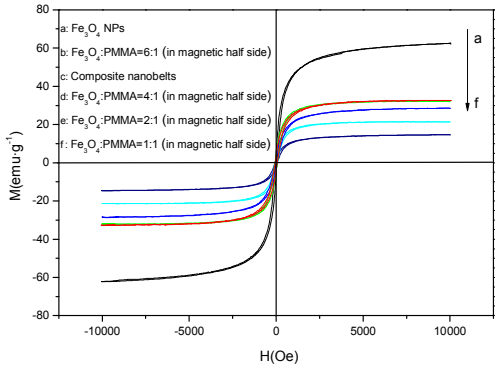

Fig. 10 Hysteresis loops of Fe_3O_4 NPs, M//F Janus nanobelts containing different mass ratios of Fe_3O_4 NPs and Fe_3O_4/Tb(BA)$_3$phen/PMMA composite nanobelts

Table 2 Saturation magnetization (Ms) of Fe_3O_4 NPs, M//F Janus nanobelts containing different mass ratios of Fe_3O_4 NPs and Fe_3O_4/Tb(BA)$_3$phen/PMMA composite nanobelts

Samples	Ms/emu·g^{-1}
Fe_3O_4 NPs	62.66
Janus nanobelts (Fe_3O_4:PMMA=6:1 in magnetic half side)	32.61
Janus nanobelts (Fe_3O_4:PMMA=4:1 in magnetic half side)	28.61
Janus nanobelts (Fe_3O_4:PMMA=2:1 in magnetic half side)	21.42
Janus nanobelts (Fe_3O_4:PMMA=1:1 in magnetic half side)	14.63
Composite nanobelts	32.15

Conclusions

In summary, novel magnetic-fluorescent bifunctional M//F Janus nanobelts with asymmetry dual-sided structure was successfully synthesized via electrospinning technique using specifically designed spinneret. The width of the Janus nanobelts is ca. 15 μm and the thickness is less than 1 μm. One half side of the Janus nanobelts is composed of Fe_3O_4 NPs and PMMA, and the other half side consists of Tb(BA)$_3$phen complex and PMMA. It is very gratifying to see that the magnetic-fluorescent bifunctional Janus nanobelts simultaneously possess both high fluorescent intensity and saturation magnetization. Compared with the simply-mixed Fe_3O_4/Tb(BA)$_3$phen/PMMA composite nanobelt which suffered the heavy loss in fluorescent emission intensity due to the existence of the everywhere dispersed Fe_3O_4 NPs, the impact of the Fe_3O_4 on the fluorescent emission intensity of the Janus nanobelts is significantly decreased. Furthermore, the color, fluorescent intensity and magnetism can be tuned via adjusting the diversity and content of fluorescent compounds and the content of magnetic compound. More importantly, the design conception and construct technique of the Janus nanobelts are of universal significance for fabricating other multifunctional Janus nanobelts, such as electrical-magnetic, photoluminescent-electrical and photoluminescent-electrical-magnetic twi- or trifunctional Janus nanobelts. The Janus nanobelts are also of significance in the development of the future nanodevice.

Acknowledgments

This work was financially supported by the National Natural Science Foundation of China (NSFC 50972020, 51072026), Ph.D. Programs Foundation of the Ministry of Education of China (20102216110002, 20112216120003), the Science and Technology Development Planning Project of Jilin Province (Grant Nos. 20130101001JC, 20070402, 20060504), the Research Project of Science and Technology of Department of Education of Jilin Province "11th 5-year plan" (Grant Nos. 2010JYT01), Key Research Project of Science and Technology of Ministry of Education of China (Grant No. 207026).

Notes and references

Key Laboratory of Applied Chemistry and Nanotechnology at Universities of Jilin Province, Changchun University of Science and Technology, Changchun 130022. Fax: 86 0431 85383815; Tel: 86 0431 85582574; E-mail: dongxiangting888@163.com

1 Y. Chen, H. R. Chen, S. J. Zhang, F. Chen, L. X. Zhang, J. M. Zhang, M. Zhu, H. X. Wu, L. M. Guo, J. W. Feng and J. L. Shi, *Adv. Funct.*

Nanoscale Accepted Manuscript

This journal is © The Royal Society of Chemistry [year]

Mater., 2011, **21**, 270-278.
2 K. Li, D. Ding, D. Huo, K. Y. Pu, Ngo Nguyen Phuong Thao, Y. Hu, Z. Li and B. Liu, *Adv. Funct. Mater*., 2012, **22**, 3107-3115.
3 P. Sun, H. Y. Zhang, C. Liu, J. Fang, M. Wang, J. Chen, J. P. Zhang, C. B. Mao and S. K. Xu, *Langmuir*, 2010, **26**, 1278-1284.
4 P. Lu, J. L. Zhang, Y. L. Liu, D. H. Sun, G. X. Liu, G. Y. Hong and J. Z. Ni, *Talanta*, 2010, **83**, 450-457.
5 D. Nagao, M. Yokoyama, N. Yamauchi, H. Matsumoto, Y. Kobayashi and M. Konno, *Langmuir*, 2008, **24**, 9804-9808.
6 W. Wang, M. Zou and K. Z. Chen, *Chem. Commun.*, 2010, **46**, 5100-5102.
7 J. Feng, S. Y. Song, R. P. Deng, W. Q. Fan and H. J. Zhang, *Langmuir*, 2010, **26**, 3596-3600.
8 H. Y. Chen, D. C. Colvin, B. Qi, T. Moore, J. He, O. T. Mefford, F. Alexis, J. C. Gore and J. N. Anker, *J. Mater. Chem.,* 2012, **22**, 12802-12809.
9 Z. Y. Zhang, C. L. Shao, X. H. Li, Y. Y. Sun, M. Y. Zhang, J. B. Mu, P. Zhang, Z. C. Guo and Y. C. Liu, *Nanoscale*, 2013, **5**, 606-618.
10 Z. Y. Liu, D. D. Sun, P. Guo and J. O. Leckie, *Nano Lett.*, 2007, **7**, 1081-1085.
11 P. Gupta and G. L. Wilkes, *Polymer*, 2003, **44**, 6353-6359.
12 W. Sambaer, M. Zatloukal and D. Kimmer, *Chem. Eng. Sci.,* 2011, **66**, 613-623.
13 J. M. Corres, Y. R. Garcia, F. J. Arregui and I. R. Matias, *IEEE Sens. J.,* 2011, **11**, 2383-2387.
14 N. A. M. Barakat, F. A. Sheikh, S. S. Al-Deyab, I. S. Chronakis and H. Y. Kim, *Sci. Adv. Mater.,* 2011, **3**, 730-734.
15 S. L. Chen, H. Q. Hou, F. Harnisch, S. A. Patil, A. A. Carmona-Martinez, S. Agarwal, Y. Y. Zhang, S. Sinha-Ray, A. L. Yarin, A. Greiner and U. Schröder, *Energy Environ. Sci.,* 2011, **4**, 1417-1421.
16 J. Song, M. L. Chen, M. B. Olesen, C. X. Wang, R. Havelund, Q. Li, E. Q. Xie, R. Yang, P. Bøggild, C. Wang, F. Besenbacher and M. D. Dong, *Nanoscale*, 2011, **3**, 4966-4971.
17 W. Wang, Z. Y. Li, X. R. Xu, B. Dong, H. N. Zhang, Z. J. Wang, C. Wang, R. H. Baughman and S. L. Fang, *Small,* 2011, **7**, 597-600.
18 H. G. Wang, Y. X. Li, L. Sun, Y. C. Li, W. Wang, S. Wang, S. F. Xu and Q. B. Yang, *J. Colloid Interf. Sci.,* 2010, **350**, 396-401.
19 Q. L. Ma, W. S. Yu, X. T. Dong, J. X. Wang, G. X. Liu and J. Xu, *J. Nanopart. Res.,* 2012, **14**, 1203-1209.
20 Q. L. Ma, J. X. Wang, X. T. Dong, W. S. Yu, G. X. Liu and J. Xu, *J. Mater. Chem.,* 2012, **22**, 14438-14442.
21 Q. L. Ma, W. S. Yu, X. T. Dong, J. X. Wang, G. X. Liu and J. Xu, *Opt. Mater.,* 2013, **35**, 526-530.
22 T. Nisisako, T. Torii, T. Takahashi and Y. Takizawa, *Adv. Mater.,* 2006, **18**, 1152-1156.
23 K. H. Roh, D. C. Martin and J. Lahann, *Nat. Mater.,* 2005, **4**, 789-763.
24 I. Salib, X. Yong, E. J. Crabb, N. M. Moellers, G. T. McFarlin, IV, O. Kuksenok and A. C. Balazs, *ACS Nano,* 2013, **7**, 1224-1238.
25 M. M. Moghani and B. Khomami, *Soft Matter,* 2013, **9**, 4815-4821.
26 Y. Y. Zheng, X. B. Wang, L. Shang, C. R. Li, C. Cui, W. J. Dong, W. H. Tang and B. Y. Chen, *Matter. Charact.*, 2011, **61**, 489-492.
27 S. B. Meshkova, *J. Fluoresc.,* 2000, **10**, 333-337.
28 B. Vazquez, S. Deb and W. Bonfield, *J. Mater. Sci.: Mater. Med.*, 1997, **8**, 455-460.
29 C. X. Du, L. Ma, Y. Xu and W. L. Li, *J. Appl. Polym. Sci.,* 1997, **66**, 1405-1410.
30 H. Zhang, H. W. Song, H. Q. Yu, S. W. Li, X. Bai, G. H. Pan, Q. L. Dai, T. Wang, W. L. Li, S. Z. Lu, X. G. Ren, H. F. Zhao and X. G. Kong, *Appl. Phys. Lett.*, 2007, **90**, 103103-103103-3.
31 R. Bonzanini, D. T. Dias, E. M. Girotto, E. C. Muniz, M. L. Baesso, J. M. A. Caiut, Y. Messaddeq, S. J. L. Ribeiro, A. C. Bento and A. F. Rubira, *J. Lumin.*, 2006, **117**, 61-67.
32 Q. Gao, G. Y. Hong, J. Z. Ni, W. D. Wang, J. K. Tang and J. B. He, *J. Magn. Magn. Mater.,* 2009, **321**, 1052-1057.
33 G. Q. Gai, L. Y. Wang, X. T. Dong, C. M. Zheng, W. S. Yu, J. X. Wang and X. F. Xiao, *J. Nanopart. Res.,* 2013, **15**, 1539-1547.
34 Q. L. Ma, J. X. Wang, X. T. Dong, W. S. Yu and G. X. Liu, *Chem. Eng. J.,* 2013, **222**, 16-22.

Nanoscale Accepted Manuscript

Graphical Abstract

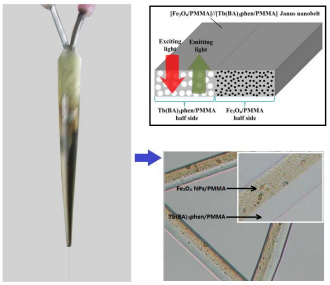

Janus nanobelts with enhanced magnetic-fluorescent bifunctional performance have been successfully fabricated by specially designed parallel spinneret electrospinning technology.

Nanoscale Accepted Manuscript